^{13}C n.m.r. studies of the thermal behaviour of aqueous solutions of cellulose ethers*

Roger N. Ibbett†, Kevin Philp and Duncan M. Price
Courtaulds Research, PO Box 111, Lockhurst Lane, Coventry CV6 5RS, UK
(Received 20 September 1991; revised 11 May 1992; accepted 12 May 1992)

Solution state n.m.r. techniques have been used to study 10% w/v aqueous solutions of methylcellulose, hydroxypropylcellulose and hydroxypropylmethylcellulose. ^{13}C n.m.r. spectra taken at temperatures from ambient to 70°C show loss of peak intensities of both backbone and substituent signals due to liquid/solid phase separation processes at high temperatures. The substituents on methylcellulose become immobile and those on hydroxypropylcellulose retain mobility. This information is interpreted on the basis of the different structures of the solid phases and the thermodynamics of the phase separation process.

(Keywords: ^{13}C n.m.r.; thermal behaviour; cellulose ethers)

INTRODUCTION

Cellulose ethers are a class of biopolymers synthesized by derivatization of cellulose pulp. Of the main types which are made commercially, hydroxypropylcellulose (HPC), methylcellulose (MC) and hydroxypropylmethylcellulose (HPMC) derivatives are the most common[1]. The degree of substitution (*DS*) of substituents can be varied over a wide range of values giving a large number of commercial grades[2]. Hydroxypropylation and methylation can occur either at glucose 2, 3 or 6 hydroxyl positions. In the case of hydroxypropylation it can also take place at the terminal substituent hydroxyl position[3], giving rise to chains more than one unit long. Also, if methylation occurs after hydroxypropylation then methyl endcapping of hydroxypropyl (HP) substituents can occur. The derivatization reactions are heterogenous, requiring the diffusion of reactants into the mercerized cellulose structure. It has always been believed that the resulting hydroxyl availabilities lead to blocks of tri-substituted glucose units, interspaced by more lightly di-, mono- and unsubstituted units[4].

The combination of the hydrophobicity of the HP and methyl (OMe) substituents and the blocky character of the final products is believed to be responsible for the unique solution properties of this class of materials[5]. MC exhibits thermogelation behaviour in water, forming a true solution at ambient temperatures and a coherent gel at elevated temperatures[6], beyond a well defined gel point (T_{gel}). HPC on the other hand forms a solution at ambient temperatures which becomes opaque beyond a definable cloud point (T_{cloud}), but does not have any gel-like characteristics[7]. Both clouding and gelation processes are completely reversible, but with MC there is a negative hysteresis between the rising and falling transition temperatures[8]. Mixed HPMC materials have intermediate behaviour, OMe-rich derivatives having recognizable gel points and HP-rich materials often displaying both an initial T_{gel} and a subsequent T_{cloud} at higher temperatures. In addition some derivatives, especially HP-rich types, show a syneresis effect whereby the gel that forms at elevated temperatures contracts with time giving rise to a pure water phase and a coherent polymer-rich solid with reduced dimensions[9].

In this study, the use of variable temperature solution state ^{13}C n.m.r. spectroscopy has been investigated as a tool for directly characterizing the thermal properties of HPC, MC and HPMC materials in aqueous solutions. Combinations of solid state ^{1}H n.m.r. magic angle spinning and ^{13}C cross-polarization/magic angle spinning methods have been employed to study thermogelling polymer systems by other workers[10,11]. However, cellulose ether gels and precipitates are severely disrupted by the high centripedal forces generated during high speed sample spinning and such techniques are therefore not appropriate. Established ^{13}C methods have been widely applied for the determination of *DS* values and chain lengths of substituents of many classes of cellulose ethers[12–16]. These rely on the different chemical shifts of the substituent carbons as compared to the glucose ring carbons, and also the changes in the shifts of the ring carbons, which are induced either by direct attachment of the substituents or attachment on neighbouring carbons. We have now extended these solution state methods by taking advantage of the additional sensitivity of carbon T_2 relaxation times to molecular tumbling rates[17]. Rochas *et al.* have used a similar approach to study the synergistic behaviour of mixed carrageenan and galactomannan solutions[18].

Conventional Fourier transform n.m.r. spectroscopy is carried out by applying radio frequency pulses to the sample to excite the n.m.r. transitions of all the chemical environments of the nucleus in question. Both longitudinal and transverse magnetization is generated which decays exponentially with time between pulses. The transverse magnetization free induction decay is observed by phase-sensitive detection and is subsequently transformed to give a frequency domain spectrum. The

* Presented at 'Physical Aspects of Polymer Science', 9–11 September 1991, University of Leeds, UK
† To whom correspondence should be addressed

0032-3861/92/194087-08

rate of free induction decay is characterized by the time constant T_2, which has long values leading to narrow spectral peaks for species with rapid tumbling rates. As molecular tumbling slows, for example during gel or precipitate formation, T_2 becomes shorter and peaks become correspondingly broader. In sufficiently slow moving materials T_2 is so short that the free induction decay is complete within the deadtime of the detector and hence no signal is observed[19]. Therefore one would expect a change in both ^{13}C n.m.r. peak widths and intensities as either thermal gelation or thermal precipitation proceeds, combined with the existing chemical shift distinction between substituent and ring carbons. The following results demonstrate the usefulness of this combined approach for the study of a series of MC, HPC and HPMC materials.

EXPERIMENTAL

Samples

Three commercially available and two laboratory prepared cellulose ether samples were used. Celacol MM10 and M20 methylcelluloses were obtained from Courtaulds PLC and Klucel E hydroxypropylcellulose was obtained from Hercules Corp. A lightly substituted methylcellulose (MC90) was synthesized by laboratory scale heterogeneous reaction with methyl chloride and a heterosubstituted hydroxypropylmethylcellulose (DP335) was similarly synthesized by reaction with methyl chloride and propylene oxide.

Thermal and physical analysis

T_{gel} and T_{cloud} values were measured on 2% w/v aqueous solutions. Solutions of all five samples were made up in boiling tubes which were then heated from ambient temperature on a water bath. The T_{gel} was defined as the temperature at which perceptible resistance to manual stirring was detected. The T_{cloud} was defined as the temperature at which visual clarity was lost through the boiling tube. The physical forms of the gels were defined approximately as falling within either weak, medium or strong categories. Approximate degrees of polymerization (*DP* values) were calculated by comparing the dilute solution viscosities with those of standards using an Ostwald viscometer[20].

N.m.r. spectroscopy

The 10% w/v solutions were made up from the five samples using deuterowater *in situ* in 10 mm o.d. high resolution n.m.r. tubes. After stirring to aid homogenization the solutions were left overnight at 5°C in order to achieve complete dissolution. The resulting solutions were centrifuged at 1400 rev min^{-1} to remove all air bubbles from the tubes prior to insertion in the n.m.r. spectrometer. All measurements were carried out on a Bruker AC300 pulsed spectrometer at a carbon frequency of 75 MHz. A capillary tube containing a solution of 3 mg ml^{-1} $Cr(acac)_3$ relaxation agent in proteo-dimethylsulphoxide (DMSO) was held coaxially in the n.m.r. tubes with the aid of a plastic collar. This separate solution was employed to provide an intensity reference signal, which would eliminate errors due to temperature-induced changes in Boltzmann n.m.r. populations. Quantitative polymer ^{13}C intensities could therefore be determined at all temperatures.

An inverse gated proton decoupling pulse sequence was used to acquire ^{13}C spectra at temperatures from ambient to 70°C. Nuclear Overhauser enhancements were suppressed by this method and a recovery delay of 5 s was used to ensure full relaxation of longitudinal magnetization between pulses. A 90° carbon pulse flip angle was employed and data were collected into a 16k file, giving a final digital resolution of 1 Hz per point. It was estimated that the full deadtime of the spectrometer under the experimental conditions used was ~100 μs, indicating that signals resulting from carbons with a T_2 less than this would not be observed. Separate inversion recovery T_1 relaxation time determinations were carried out on the observable fractions of a 10% solution of sample MM10, both at ambient and at 60°C. The maximum T_1 values found were for the substituent methyl carbons, which were 0.41 and 1.2 s, respectively.

Before all measurements the temperature was stabilized for ~15 min. In most cases 1000 acquisitions were accumulated at each temperature, but some measurements were carried out overnight resulting in up to 14 000 acquisitions. One isothermal experiment was carried out at 70°C, using the DP335 HPMC sample. Ten spectra were measured consecutively, over a period of 12 h, each resulting from 1000 acquisitions. This was designed to examine changes in gel spectral intensities which might occur due to syneresis after long periods at elevated temperatures.

RESULTS AND DISCUSSION

Table 1 shows the molar substitution of HP units, the *DS* of OMe and HP substituents and HP chain lengths for the five samples. These values were determined by separate analysis of solution state ^{13}C spectra of acid

Table 1 Thermal and physical data for MC, HPC and HPMC aqueous solutions

Material	Type	Methyl	Hydroxypropyl				T_{gel}	T_{cloud}	Gel
		DS	*MS*[b]	*R*[c]	*DS*	*DP*[a]	(°C)	(°C)	type
MM10	MC	1.9				~60	45	54	Firm
M20	MC	1.6				~75	48	60	Firm
MC90	MC	1.1				~90	–	–	Weak
Klucel E	HPC	–	5.9	2.1	2.8	~250	–	45	No gel
DP335	HPMC	1.4	0.21	1.4	0.15	~80	–	72	Very weak Gel

[a] Based on Table 7 in ref. 27 and Table III in ref. 28
[b] Average molar substitution
[c] Average HP chain length

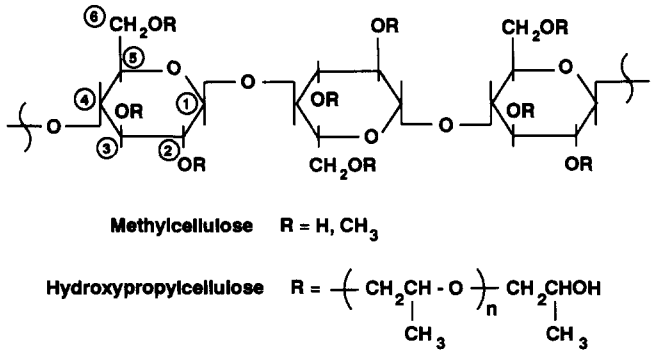

Figure 1 Typical molecular structures of methylcellulose and hydroxypropylcellulose

Table 2 ^{13}C chemical shifts of methylcellulose and hydroxypropylcellulose in deuterowater[3,13] referenced against an external chemical shift reference of DMSO at 40 ppm

Carbon types	^{13}C chemical shifts		
	MC	HPC	HPMC
C_1	100	100	100
$C_{2s,3s}$	80–81	79–82	79–82
C_4	76	76	76
C_{2-5}	70–74	74–76	70–76
$C_{6\text{-OMe}}$	68		68
$C_{6\text{-HP}}$		70	70
C_6	57	57	57
OMe-6	58		58
OMe-3	56.5		56.5
OMe-2	56		56
HP–CH internal		73.5	73.5
HP–CH end		64–65	64–65
HP–CH_2 internal		74	74
HP–CH_2 end		72	72
HP–CH_3 end		16.5	16.5
HP–CH_3 internal		14	14

hydrolysates, some of the assignments being made by reference to model polymers[3,14]. Typical structures are shown in *Figure 1*. *Table 1* also shows T_{gel} and T_{cloud} values, as determined by classical thermal measurements, and simple classifications of gel types. The average *DP* values for all samples are also shown, determined by viscosity measurements[2]. The ^{13}C chemical shifts of the different carbon types are shown in *Table 2*.

Figure 2 shows the ^{13}C spectrum of MM10 at ambient temperature and at 70°C. As can be seen the C_1, C_{2-5} and OMe+C_6 resonances are sufficiently resolved for the determination of peak areas at all temperatures. Careful note was made of any possible confusion in the OMe substituent intensity that might be caused by the presence of the hidden C_6 peak in the same region. The resulting plots of the areas of C_1 and OMe peaks of MM10, M20 and MC90 samples against temperature are shown in *Figure 3*. Intensity increases are seen at temperatures slightly above ambient, which is associated with a thermally induced reduction in solution viscosity. Although the macroscopic solution viscosity would not be expected to change by very much, there is a noticeable decrease in ^{13}C peak widths at temperatures slightly above ambient, especially near the peak baselines. This confirms that there is an increase in molecular scale polymer mobility, giving rise to an increase in T_2 relaxation times, and the redistribution of intensity from the peak wings in the peak centre. Thus, less signal intensity is lost both during the deadtime of the detector and also in the baseline noise. However, as the temperature is raised further, all plots indicate an increasing loss of intensity of all peaks. This is interpreted as a loss in polymer backbone and methyl substituent mobility indicating that gelation has occurred, with more polymer material becoming involved in gel structures at higher temperatures. Course temperature intervals were required

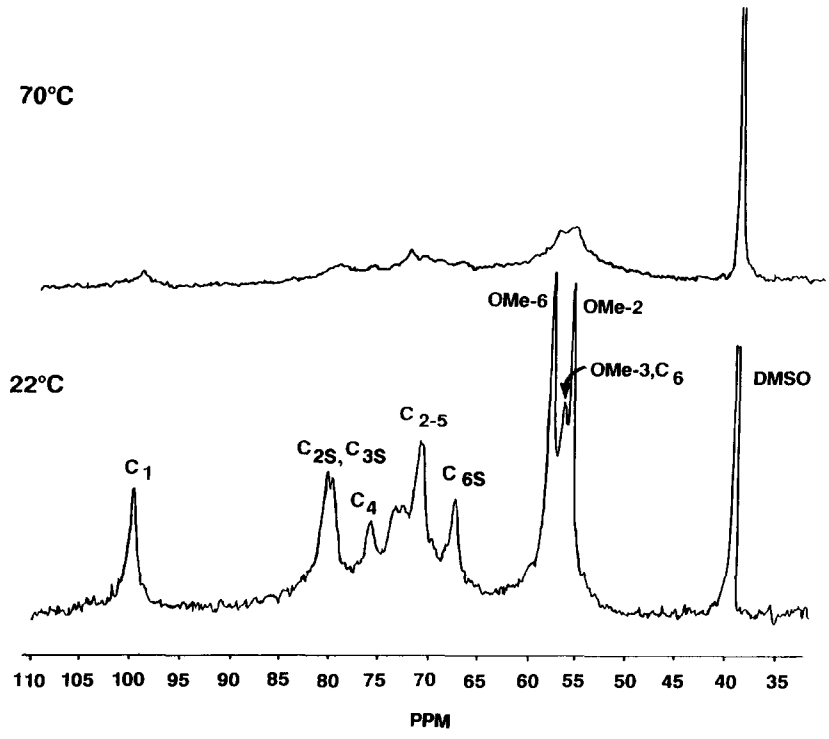

Figure 2 ^{13}C spectra recorded at 70°C and 22°C of a 10% w/v solution of MM10 methylcellulose in D_2O. Peak at 40 ppm is of the proteo-DMSO external standard in the coaxial capillary tube, which also contained 3 mg ml^{-1} $Cr(AcAc)_3$ relaxation agent. The spectral intensities have been normalized to that of DMSO

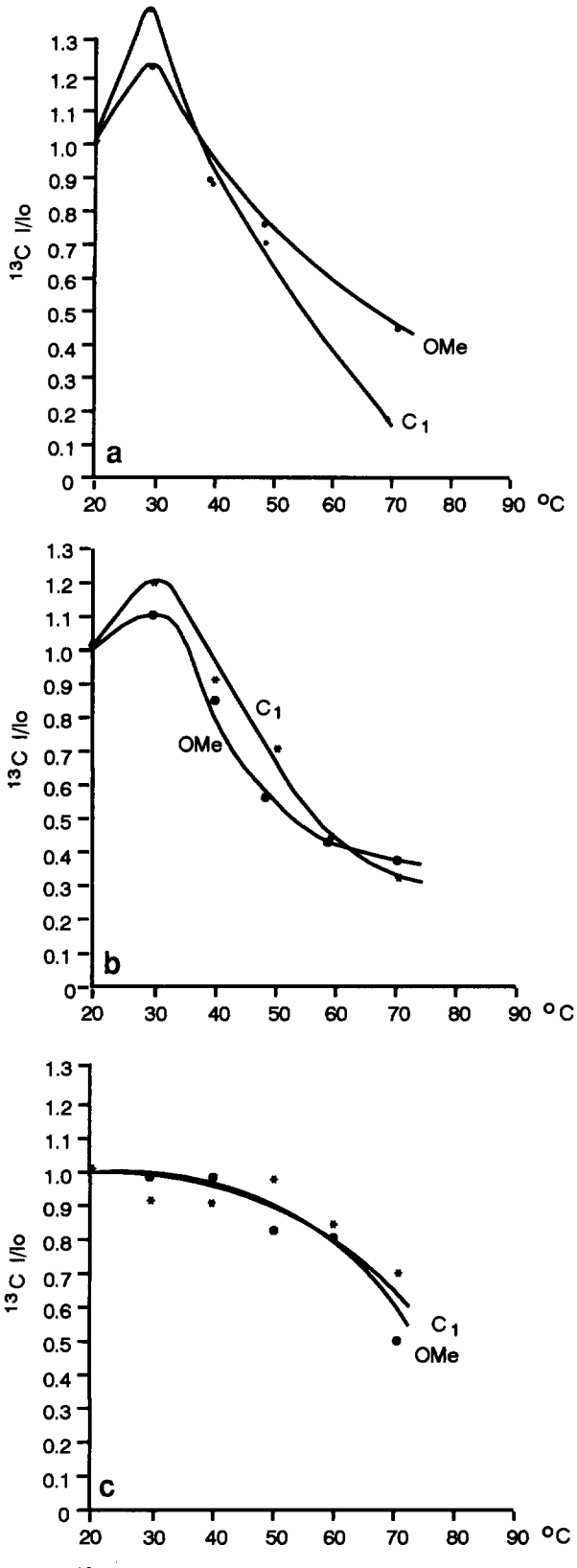

Figure 3 ^{13}C intensities of C_1 and OMe signals of 10% w/v solutions of methylcellulose in D_2O at different temperatures. In each case intensities were first normalized agsinst that of an external DMSO standard normalized and then against the intensity of the signal at 22°C: (a) MM10; (b) M20; (c) MC90

to compensate for the long spectral accumulation times, which make determination of an accurate gel temperature difficult by the n.m.r. method, so no attempt was made at correlation with data determined classically at 2% concentrations.

It is noted again that n.m.r. is sensitive to molecular scale motion, whilst viscosity measurements are sensitive to bulk polymer motion, and hence the two techniques are not observing exactly the same phenomena. The three plots in *Figure 3* show that there are less obvious agreements between onset of intensity loss and *DS* than determined classically, this being at ~35°C for MM10 and ME20 and 45°C for MC90. This may provide evidence that the corresponding onset of change at a molecular level is not as temperature dependent. The intensity loss is greatest for the highest substituted MM10 sample, the backbone intensity falling to ~17% of the original value at 70°C, as compared with 30% for the M20 sample and 65% for the MC90 sample. At higher temperatures there is also an indication that methyl substituent intensity is retained to a greater extent, especially in the case of the MM10 sample. This is probably because the internal rotational motion around the methyl axis is not as restricted as for the backbone carbons, especially in the less coherent regions of the gel. Applying the reverse argument, this could be interpreted as evidence that in M20 a greater fraction of the total number of methyl substituents is attached to units in coherent gel regions than in MM10. The loss in OMe substituent intensity in general follows the loss in backbone intensity, although the OMe intensity maxima at the onset of intensity loss are lower than those for the C_1 peaks in both the MM10 and M20 plots. This could be interpreted as evidence that high methyl content regions of the polymers are involved in the initial stages of gel formation. It must be noted that in case of MC90 only 70% of the polymer gave rise to detectable ^{13}C signals at ambient temperatures, suggesting that some polymer segments were completely unsubstituted and therefore insoluble. The classical thermal analysis of a 2% solution of this sample revealed that it formed a weak gel.

Figure 4 shows ^{13}C spectra of Klucel E, taken at ambient and 70°C. Comparison of the spectra clearly shows that HP substituent resonances retain intensity even at temperatures well above the T_{cloud} of the solution, unlike the backbone resonances which are significantly reduced. This is illustrated in more detail in *Figure 5*, which shows the change in areas of the C_1, internal and end HP methyl peaks with temperature. The end HP methyl intensity is almost unchanged by the clouding phenomenon, indicating that although solid material has formed the substituent ends are moving freely in the solvent. The internal HP methyl intensity is lost to some extent, the integrals of internal and end methyl peak areas giving an effective substituent chain length of 1.6 as opposed to the true value of 2.1. This is consistent with the loss of backbone mobility, which has an onset at ~40°C and leads to progressively more polymer chains becoming immobilized, up to a temperature of 70°C. The rigidity of the polymer backbones also reduces the mobility and subsequently the signal intensity of some of the adjacent internal HP substituents.

Charlet *et al.*[7,20] have suggested that aqueous solutions of HPC precipitate to form a rigid cholesteric solid phase at high temperatures, where the cellulose backbones are arranged in supramolecular helical structures. This solid polymer phase coexists with a dilute liquid phase. While the existence of a solid precipitate is borne out by the n.m.r. results, they also indicate that the polymer is sufficiently loosely agglomerated to allow the HP substituents full freedom of motion in the solution. It therefore

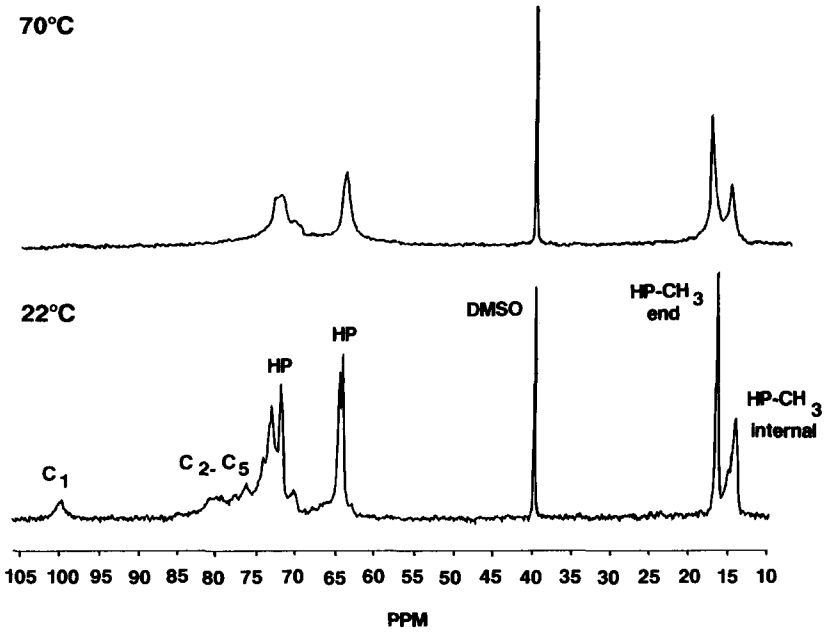

Figure 4 ^{13}C spectra recorded at 70°C and 22°C of a 10% w/v solution of Klucel E hydroxypropylcellulose in D_2O. Peak at 40 ppm is of the proteo-DMSO external standard in the coaxial capillary tube, which also contained 3 mg ml^{-1} $Cr(AcAc)_3$ relaxation reagent. The spectral intensities have been normalized to that of DMSO

also follows that the substituents are still fully solvated, contrary to theories suggesting that HP dehydration is the driving force that promotes phase separation[20,21]. However, Sandell and Goring[22,23] report that dilute aqueous solutions of propylene oxide, dimers, trimers and pentamers remain clear at all temperatures and show no sign of phase separation. The average chain lengths of the HP substituents in this Klucel E sample are of a similar order, which lends further support to the current n.m.r. view that they would remain in solution at all temperatures.

Kato *et al.*[6] have proposed that MC undergoes gelation by formation of 'crosslinking loci' which consist of small crystallites of trimethylcellulose. Runs of tri-substituted cellulose units are believed to be formed as a natural consequence of the heterogeneous reaction conditions used to synthesize MC from cellulose pulp[5]. At high temperatures runs from different polymer chains can crystallize together, and if each polymer chain goes through several crystallites then this will result in the creation of a three-dimensional polymer network. The mechanical properties of the high temperature MC gel phase strongly support the argument that crosslinks exist[8], whilst X-ray diffraction evidence has led to the interpretation that crystalline regions are present[6]. However, the current n.m.r. evidence demonstrates that the overriding process occurring is in fact phase separation, or precipitation, with progressively more polymer material becoming incorporated into the solid phase as the temperature is raised

Kato *et al.*[6] calculated that to form a gel only two nodes are necessary per polymer chain, and that trimethyl runs do not have to be longer than five units. Applying the same arguments, if a chain length of 100 is assumed then only 1.2% of the total polymer would be immobilized due to a phase change at the initial gel point, representing 5% of the total OMe units. This would explain why there is only a small change in the apparent *DS* at the onset of immobilization of the methyl substituents and the cellulose backbone as shown in *Figure 3*. These small differences are only marginally greater than the overall errors to be expected in the determination of peak areas, which are of the order of 10% of total peak area. The same argument explains why at highest temperatures there is limited n.m.r. evidence that only monosubstituted cellulose units are entering the solid phase.

Initial interchain phase separation of highly substituted runs of MC would create a very loose but coherent three-dimensional network, with the crosslink points acting as the seeds of further solid precipitation. The n.m.r. evidence suggests that progressively more cellulose units join the solid phase, causing the size of the initial crosslink regions to increase. As the temperature increases further precipitation would be expected to extend into the regions between cross-links, eventually causing all polymer units to coalesce into a coherent solid matrix. The final coherence is due to the initial network formation, which distinguishes the behaviour of MC from that of HPC, where no initial crosslink formation can occur.

Figure 6 shows the ^{13}C spectra of DP335 HPMC at ambient temperature and 90°C. None of the peaks appear to lose intensity at high temperature, despite the fact that the sample is above its T_{gel} and T_{cloud}. The separate 12 h isothermal experiment at 70°C confirmed that any syneresis effects that might be occurring would have no influence on the spectra. However, the expansion of the C_1 region in *Figure 7* reveals the high temperature peak to be bi-component in nature, with a small sharp peak superimposed on a much broader one. The plot in *Figure 5* shows the variation of the C_1, OMe and HP methyl peak areas with temperature, and as can be seen when the temperature is progressively increased the broad peak becomes more dominant at the expense of the sharp peak. Incipient phase separation is therefore observed by n.m.r., the new partially immobilized phase giving rise to broad underlying peaks, although clearly the rigidity

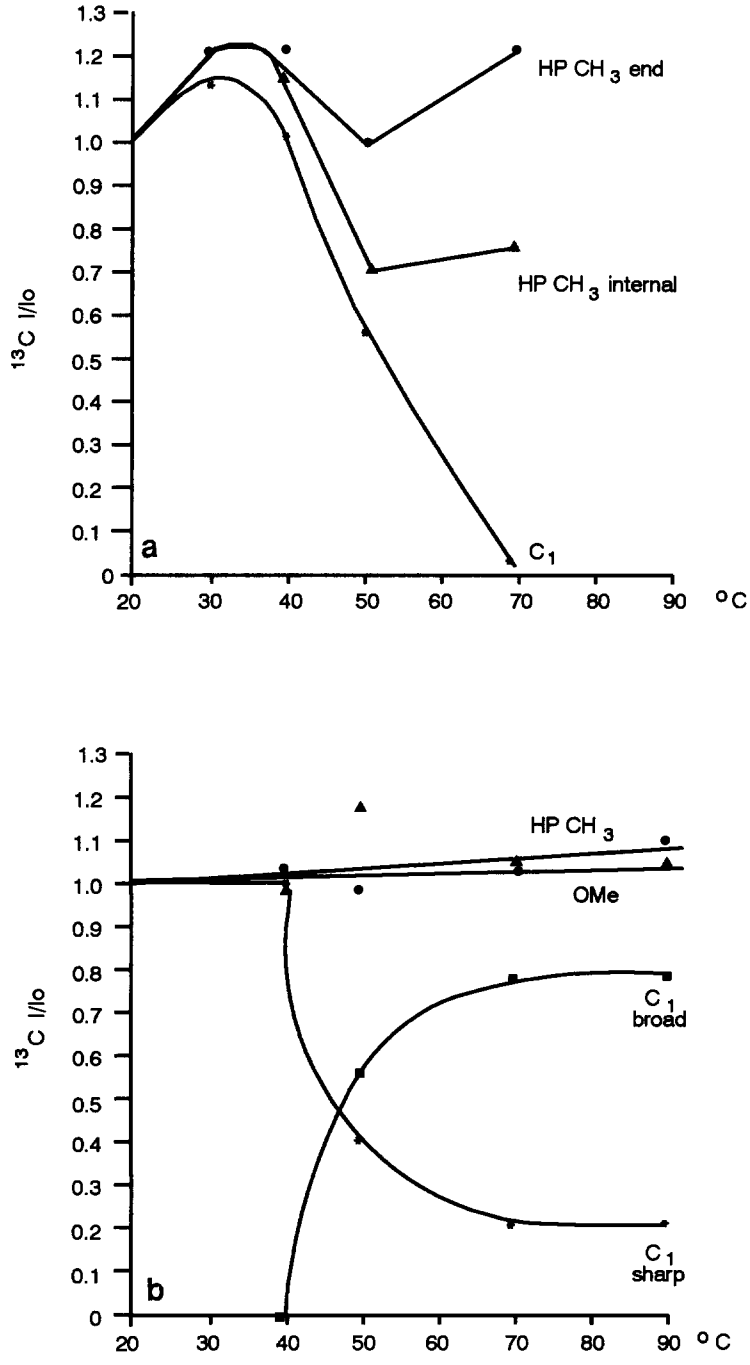

Figure 5 ^{13}C intensities of (a) the C_1, internal and end HP-Me signals of a 10% w/v solution of Klucel E hydroxypropylcellulose and (b) the C_1, total HP-Me and OMe signals of a 10% w/v solution of DP335 hydroxypropylmethylcellulose; both in D_2O, at different temperatures. In each case intensities were first normalized against that of an external DMSO standard normalized and then against the intensity of the signal at 22°C

of the backbone is insufficient to reduce the ^{13}C T_2 of the associated carbons below that of the spectrometer deadtime. The DP335 sample has a higher T_{gel} than M20 or MM10, and also gives rise to very weak gel. There must be sufficient runs of highly methylated cellulose units for interchain phase separation to occur, although presumably the achievable numbers of cross-links and their dimensions are lower because of the disruptions caused by intervening hydroxypropylated units[9]. Hydroxypropylated units will also phase separate, but the coiling of the polymer backbone will be disrupted by the presence of methylated units, leading to a more open disorganized solid phase. This is unlike the case resulting from phase separation of Klucel E, where compact, ordered structures are formed, due to the uniform distribution of substituents along the backbone. Thermodynamically, a mixed substituent system would be expected to exhibit phase separation at higher temperatures[24], due to the statistical difficulties of bringing like units together. The physical properties of the mixed substituent separated phase would be expected to have the characteristics intermediate between both homosubstituent systems.

The thermodynamic driving force behind phase separation and solid phase structuring in cellulose ethers has been the subject of a number of studies[4,6,7,20,21]. This

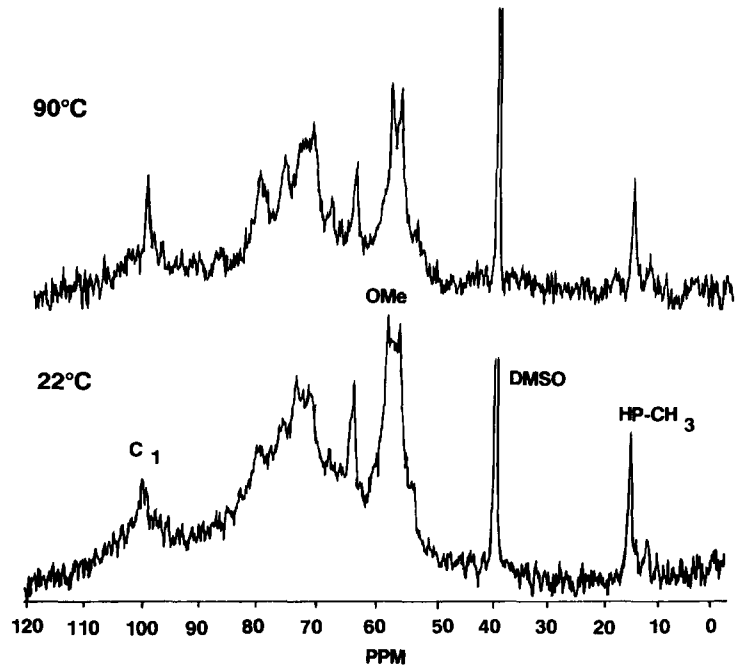

Figure 6 ^{13}C spectra recorded at 90°C and 22°C of a 10% w/v solution of DP335 hydroxypropylmethylcellulose in D_2O. Peak at 40 ppm is of the proteo-DMSO external standard in the coaxial capillary tube, which also contained 3 mg ml^{-1} $Cr(AcAc)_3$ relaxation reagent. The spectral intensities have been normalized to that of DMSO

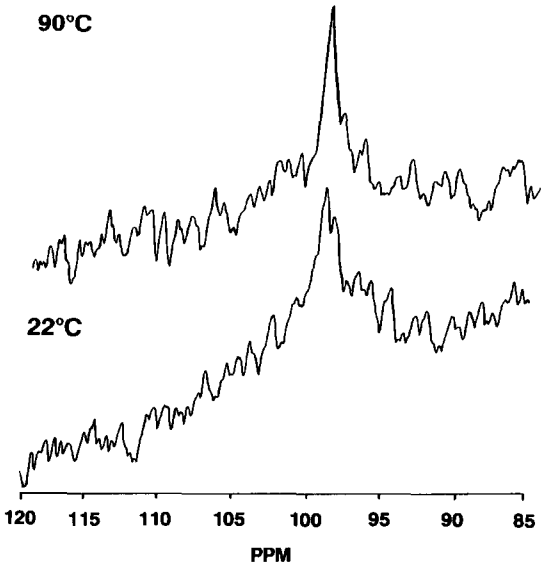

Figure 7 ^{13}C spectral expansion of *Figure 6*, C_1 region

new n.m.r. evidence provides important dynamic information on the HPC and MC polymers, lending support to some of the proposed theories. It has been established that solubility in aqueous media is conferred on the cellulose ethers as a result of a negative enthalpy of dilution ($\Delta H_d < 0$). It is proposed according to the theory of Franks[25] that water is a highly structured solvent, with individual water molecules continuously making and remaking hydrogen bonds to their neighbours. At any moment in time it can be considered that an 'ice' type morphology exists, and it is into the interstices within this dynamic structure that hydrophobic groups are most favourably positioned. The net effect is that an increase in solvent structuring occurs around the hydrophobic units, which leads to more stable hydrogen bonding in the created 'lattice' cavities, and a negative enthalpy change. This so-called hydrophobic effect also results in a negative entropy of dilution ($\Delta S_d < 0$), since the entire system including solvent and solute is more restrained, despite the fact that the dissolved polymer has more conformational freedom. A combination of negative enthalpy and negative entropy changes means that the total free energy of dilution will become positive at elevated temperature as a result of the relationship $\Delta G = \Delta H - T\Delta S$.

Our results on the MC system fully support the mechanism of phase separation at elevated temperatures. Conventional ^{13}C analysis of the glucose residues of typical MC of $DS = 1.7$ confirms that a range of glucose derivatives are present, on average 24% tri-, 43% di-, 23% mono- and 8% unsubstituted types[14,26]. Thus a range of hydrophobicities will exist along a typical polymer chain, and subsequently a range of temperatures for phase separation. In view of the confirmation of this liquid to solid phase separation mechanism, we see no need to invoke the separate crystallite formation mechanism proposed by Kato *et al.*[6] to explain the initial formation of a network. The loss of solubility of cellulose chain segments with highest substitution will result in their adoption of the most thermodynamically favourable state, which in the case of MC must be in micelles with other highly substituted segments from other polymer chains. Subsequent phase separation of less substituted segments will cause these solid regions to grow to form an open porous structure with solvent filling the voids. This we believe is the true nature of the so-called gel state at the highest temperatures used in this study. At, for example, 70°C and above a solid, sponge-like structure must exist, with only a minor fraction of the polymer still solubilized in the sponge pores.

Commercial HPC is much more highly substituted,

with consequently a much more even distribution of substituents. Water solubility is again conferred by a negative ΔH_d, as is also the case for propylene oxide oligomers. However, this study has shown that the phase behaviour of HPC is not governed by the properties of the HP substituents, it being proved that short chain length HP substituents do not undergo phase separation. The structure of the solid phase must be such that the cellulose backbones of the polymer chains are immobilized, whilst the HP substituents remain solvated. The proposal of Charlet *et al.*[7,20] that the polymer backbones coil into supramolecular cellulose helixes therefore fits well with our new data, with the refinement that the substituents project into the solvent and undergo cilia type motion. We must assume that these cilia keep adjacent cellulose coils apart, maintaining the solid phase in a highly dispersed state. Sandell and Goring[22] used a disc coil model for propylene oxide oligomers to estimate the amount of hydrophobic methyl group surface which could be buried in the interior when chains of different lengths were coiled into helixes. They found that only 17% of the hydrophobic methyl surface area could be enclosed in this way for a chain length of 2, representing a minimal reduction in unfavourable interaction with the solvent. We assume therefore that there is no thermodynamic driving force for HP substituent desolvation even though the hydrophobic effect breaks down at elevated temperatures. In addition, the high *DS* of commercial HPC means that the polymer backbone has little hydrophilic character, so it could be involved in promoting a hydrophobic effect with water. Indeed, this is a plausible explanation of why the backbone is extended and mobilized in solution. Thus it follows that at elevated temperature it is the breakdown of the backbone hydrophobic structure that leads to the adoption of a more favourable phase separated coiled structure.

CONCLUSIONS

Solution state ^{13}C n.m.r. has been proved to be an invaluable tool for studying the dynamic behaviour of cellulose ethers during the process of phase separation and gelation. It has chemical selectivity, allowing changes in substituent and backbone signals to be measured separately. The current work has clearly shown that in aqueous commercial grade MC solutions both backbone and substituents lose mobility as progressive phase separation occurs at elevated temperatures. There is some evidence that highly substituted regions separate first, and we believe that solid micelle crosslinks are formed giving rise to a three-dimensional network. Subsequent separation extends and connects these micelles, leading eventually to the formation of a porous water-filled solid. Commercial HPC undergoes a similar but more abrupt phase separation. The current work supports the conclusion that the cellulose backbones coil into supramolecular helical structures. However, importantly, the substituents remain solvated and we believe that they act as cilia projecting outwards from the coiled backbone into the solvent. This keeps adjacent coils apart leading to a very loose, open precipitate with no gel-like properties.

REFERENCES

1 Davidson, R. L. (Ed.) 'Handbook of Water-soluble Gums and Resins' McGraw Hill, New York, 1980
2 Celacol Technical Manual, Courtaulds Chemicals, Water Soluble Polymers, Spondon, 1988
3 Kimura, K., Shigemura, T., Kubo, M. and Yasumitsu, M. *Makromol. Chem.* 1985, **186**, 61
4 Takahashi, S., Fujimoto, T., Miyamoto, T. and Inagaki, H. *J. Polym. Sci., Polym. Chem. Edn* 1987, **25**, 987
5 Just, E. K. and Majewicz, T. G. in 'Encyclopedia of Polymer Science and Engineering', Vol. 3, 2nd Edn, Wiley, New York, 1985, pp. 226–269
6 Kato, T., Yokoyama, M. and Takahashi, A. *Colloid Polym. Sci.* 1978, **265**, 15
7 Fortin, S. and Charlet, G. *Macromolecules* 1989, **22**, 2286
8 Klug, E. D. *J. Polym. Sci. C* 1971, **36**, 491
9 Sarkar, N. *J. Appl. Polym. Sci.* 1979, **24**, 1073
10 Badiger, M. V., Rajamohanan, P. R., Kulkarni, M. G., Ganapathy, S. and Mashelkar, R. A. *Macromolecules* 1991, **24**, 106
11 Gidley, M. *Macromolecules* 1989, **22**, 351
12 Ho, F., Kohler, R. and Ward, G. A. *Anal. Chem.* 1972, **44**, 178
13 Parfondry, A. and Perlin, A. S. *Carbohydrate Res.* 1977, **57**, 39
14 Gronski, W. and Hellman, G. 'Proceedings of the International Dissolving Pulps Conference', TAPPI, Atlanta, 1987, p. 167
15 Isogai, A., Ishizu, A. and Nakano, J. *J. Appl. Polym. Sci.* 1986, **31**, 341
16 Zadorecki, P., Hjertberg, T. and Arwidsson, M. *Makromol. Chem.* 1987, **188**, 513
17 Doskocilova, D., Schneider, B. and Jakes, J. *J. Mag. Res.* 1978, **29**, 79
18 Rochas, C., Taravel, F.-R. and Turquois, T. *Int. J. Biol. Macromol.* 1990, **12**, 353
19 Fukushima, E. and Roeder, S. B. W. 'Experimental Pulse NMR', Addison-Wesley, Reading, MA, USA, 1981
20 Robitaille, L., Turcotte, N., Fortin, S. and Charlet, G. *Macromolecules* 1991, **24**, 2413
21 Winnik, F. M. *Macromolecules* 1987, **20**, 2745
22 Sandell, L. S. and Goring, D. A. I. *J. Polym. Sci. A2* 1971, **9**, 115
23 Sandell, L. S. and Goring, D. A. I. *Makromol. Chem.* 1970, **138**, 77
24 Flory, P. J. *J. Chem. Phys.* 1949, **17**, 223
25 Franks, F. 'Water: a Comprehensive Treatise', Vols 4–6, Plenum Press, New York, 1975–1979
26 Yalpani, M. and Reuben, J. (Eds) 'Industrial Polysaccharides. Genetic Engineering, Structure/Property Relationships and Applications', Elsevier, Amsterdam, 1987, p. 305
27 Klucel technical information, Aqualon (UK) Ltd, 1987. Benecel technical information, Aqualon (UK) Ltd, Warrington, 1991